Compressible DNS of a Low Pressure Turbine subjected to Inlet Disturbances

L.W. Chen, R. Pichler, and R.D. Sandberg

1 Introduction

In modern low pressure turbines (LPT), reducing the number of airfoils in a turbine leads to an increase in the blade loading, which inevitably increases the possibility of laminar separation. Moreover, both separation bubbles and the type/location of laminar-turbulent transition are known to be sensitive to inlet disturbances. The influence of inlet disturbances has been studied experimentally with background turbulence generated by a grid and wakes by upstream moving bars in the pitchwise direction [1, 2, 3]. The first incompressible direct numerical simulation (DNS) for a turbine cascade flow was performed by Wu and Durbin [4] using prescribed wake disturbances and it was found that incoming wakes are responsible for longitudinal structures forming on the pressure side. The same inlet conditions were later applied to additional studies using incompressible DNS and large-eddy simulations (LES) [5], which have contributed further to the understanding of the effect of incoming wakes on boundary layer characteristics. More recently, Sarkar [6] performed incompressible LES using wakes generated by a precursor simulation of a cylinder flow and showed that the structure of the incoming wakes strongly affects blade performance and wake losses.

In the current paper, we are going to look into the effect of incoming bar wakes at different reduced frequencies and its combination of inflow back-

L.W. Chen
Aerodynamics and Flight Mechanics Research Group, University of Southampton, Southampton SO17 1BJ, United Kingdom, e-mail: l.chen@soton.ac.uk

R. Pichler
Aerodynamics and Flight Mechanics Research Group, University of Southampton, Southampton SO17 1BJ, United Kingdom, e-mail: r.pichler@soton.ac.uk

R.D. Sandberg
Aerodynamics and Flight Mechanics Research Group, University of Southampton, Southampton SO17 1BJ, United Kingdom, e-mail: R.D.Sandberg@soton.ac.uk

ground turbulence, and study their influences on the blade performance and loss generation.

2 Methodology and computational details

The compressible Navier-Stokes equations for the conservative variables are solved using a DNS code. The numerical method comprises a five-step, fourth-order accurate low-storage Runge-Kutta method for the time integration, state-of-the-art parallelizable wavenumber optimized compact finite differences for the spatial discretization in the streamwise and pitchwise directions and a Fourier method using the FFTW3 library for discretization of the spanwise direction. Additionally, a skew-symmetric splitting is used to stabilize the convective terms. The inflow turbulence is generated using a synthetic turbulence generation method [7, 8]. More details about the numerical method can be found in [8].

The linear turbine cascade geometry in the present work is the T106 profile experimentally investigated by Stadtmüller [9]. 9 blocks are connected using characteristic interface conditions [8], and 864 grid points are distributed along the blade surface. In the spanwise direction, the width of the computational domain was chosen as 0.2 chord lengths and 32 Fourier modes were employed with 100% de-aliasing (using 66 collocation points in physical space), resulting in a total of 25×10^6 grid points for each simulation. The mesh resolution has been tested sufficient for DNS [8].

The isentropic Reynolds number $Re_{2is} = 60,000$ and the isentropic Mach number $M_{2is} = 0.405$ are kept the same for all cases. At the outlet boundary non-reflective characteristic boundary condition was applied. At the inlet boundary, a fixed inflow condition with an inflow angle of $\alpha = 46.1°$ was specified and a sponge layer, forcing the flow solution to a target state, was employed in the inlet region to remove unphysical acoustic waves [8]. To generate periodically incoming bar wakes, an immersed boundary method is implemented using feedback forcing terms proposed by Goldstein et al. [10]. In all the simulations, each cylinder bar at $x/C = -0.7$ contains 90 time-varying immersed boundary points with the diameter of $0.02C$ and the velocity in $y-$direction is $V_{bar} = -0.41$. Here, C is the blade chord length. Through changing the bar spacing, various reduced frequencies $F_{red} = f \cdot C/V_{2is}$ can be achieved, where f and V_{2is} are bar passing frequency and isentropic exit velocity, respectively. The cascade inlet measurement plane is at 30% chord upstream the blade leading edge and outlet measurement plane at 40% chord downstream of the trailing edge.

3 Results

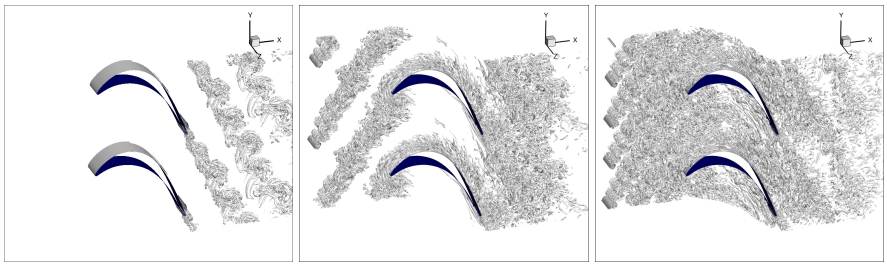

Fig. 1 Instantaneous iso-surfaces of the second invariant of the velocity-gradient tensor ($Q = 100$) for $F_{red} = 0$ (left), $F_{red} = 0.31$ (middle) and $F_{red} = 0.61$ (right).

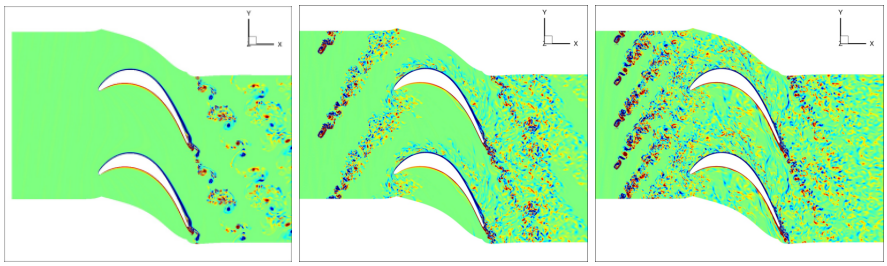

Fig. 2 Instantaneous contours of the spanwise component of vorticity (-50 to 50) for $F_{red} = 0$ (left), $F_{red} = 0.31$ (middle) and $F_{red} = 0.61$ (right).

The present study is aimed to investigate the effect of incoming bar wakes at different reduced frequencies and its combination of inflow background turbulence. Several typical cases are discussed, i.e. $F_{red} = 0$ cases with $Tu = 0\%$ and 4% (no moving bar), $F_{red} = 0.31$ case with $Tu = 0\%$, and $F_{red} = 0.61$ cases with $Tu = 0\%$ and 4%. For each case, the simulation was run for 5 pass through time in 2D, then 3D simulation was restarted from the fully developed 2D result. After about 10 pass through time, to avoid the transient period, samples were then collected for 20 bar passing periods to obtain statistically meaningful turbulence properties.

To assess the existence of coherent structures, figure 1 shows the instantaneous snapshots of $F_{red} = 0$, 0.31 and 0.61 cases (without inflow turbulence) depicted by iso-surface of the Q criterion. In the case of $F_{red} = 0$ (or clean case), laminar flow separation in the aft section of the suction side can be observed with highly spanwise coherent vortex shedding. In the $F_{red} = 0.31$ and $F_{red} = 0.61$ cases, the bar wakes generated by moving cylinders develop downstream into highly 3D structures and interact with the blade boundary

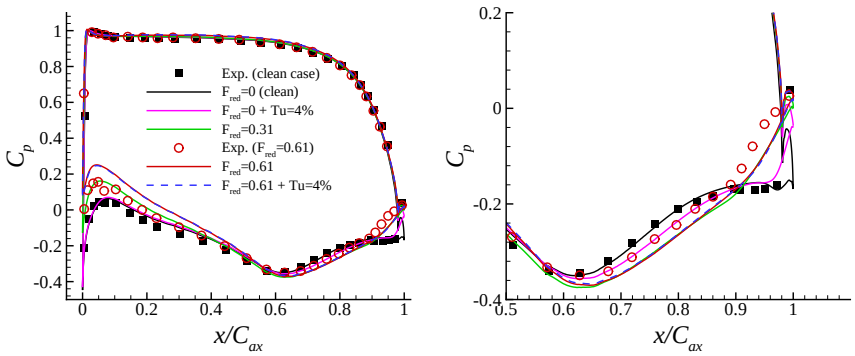

Fig. 3 Pressure coefficient distribution on the blade surface and a zoom-in view near the trailing edge. Here, C_{ax} is the axial chord length.

layers. Compared to the clean case, the wake downstream of the blade trailing edge look less spanwise coherence, which can also be seen when looking at instantaneous contours of the spanwise vorticity component in figure 2.

For more quantitative assessment of the effect of reduced frequency on the blade performance, the pressure coefficient C_p, is compared to experimental data in figure 3. A zoom-in view near the trailing edge also shows the differences. The result of the $F_{red} = 0$ case with $Tu = 0\%$ (clean case) compares well with the experimental data and the plateau near the trailing edge indicates a laminar separation bubble. For $F_{red} = 0$ with $Tu = 4\%$, the separation bubble shrinks and reattachment appears to occur further upstream with pressure rising to a larger value. Due to the movement of bars, the cascade inlet angles measured at $x/C = -0.3$ became $43.76°$ for $F_{red} = 0.31$ and $41.72°$ for $F_{red} = 0.61$, which lead to the differences from the clean case at the suction side. There is no noticeable difference between $F_{red} = 0.61$ with $Tu = 0\%$ and $Tu = 4\%$, and reasonable agreement with the experimental data is obtained. Aft the suction peak, it is clear that in the mean sense the incoming wakes suppressed the separation bubble. This finding was also confirmed in some incompressible DNS studies [5].

The stagnation pressure losses Ω are of the obvious importance in the engineering and also very challenging for DNS studies [8]. In figure 4 (a), the wake losses from all the cases are compared to the reference data. The coordinate y^* is a normalized scale in the pitchwise direction from the suction to the pressure side, defined as $y^* = \frac{(y-y_{max})}{(y_{max}-y_{min})}$. The result of $F_{red} = 0$ case with $Tu = 0\%$ matches the experimental data very well, while the $Tu = 4\%$ case shows a lower peak value and also the location of the peak moves closer to the pressure side. This can be explained by the change of the suction side separation bubble for the turbulent cases which leads to a different defect of the wake. Similar phenomena can be found for $F_{red} = 0.31$ and 0.61 cases, but the profiles of wake loss are sharper. The $F_{red} = 0.61$ case result agrees

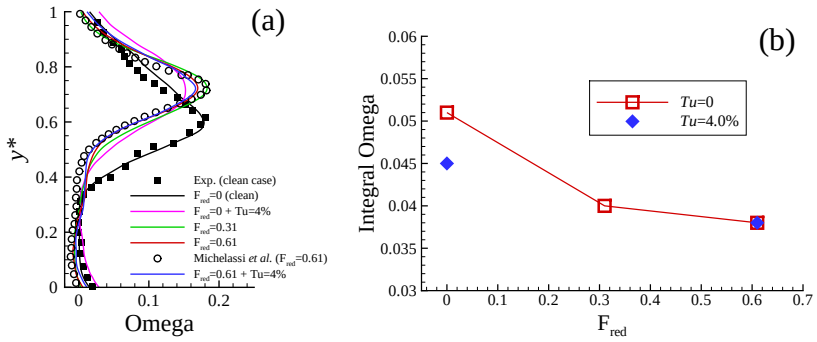

Fig. 4 Comparison of the wake stagnation pressure loss profiles with reference data (a) and the scalar integral of wake losses (b).

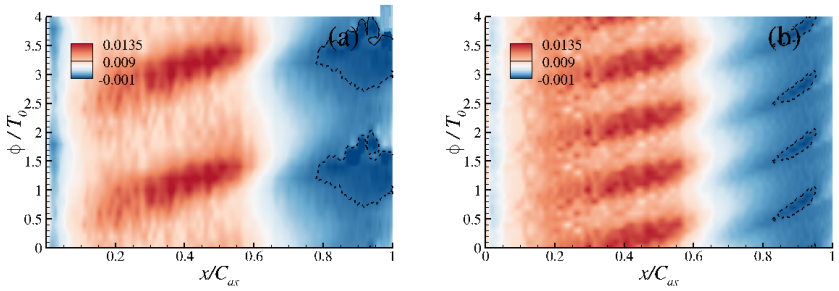

Fig. 5 Space-time diagrams of wall shear stress: (a) $F_{red} = 0.31$, $Tu = 0\%$; and (b) $F_{red} = 0.61$, $Tu = 0\%$.

well with the incompressible one by Michelassi et al. [5] and $Tu = 4\%$ does not show significant difference except a broader profile at the pressure side and slightly smaller value at the suction side.

A scalar integral over pitchwise direction has been done for each wake loss profile in order to study the overall losses at different reduced frequencies. Figure 4 (b) shows the scalar integral wake losses versus three reduced frequencies. With the increment of reduced frequency, the wake loss is dramatically reduced. Also, the influence of the inflow turbulence level is less significant in $F_{red} = 0.61$ case.

To better understand the physical process in the moving bar cases, the phase-averaged statistics have been collected during 30 bar passing periods for $F_{red} = 0.31$ and 0.61 ($Tu = 0\%$). Each period is divided into 10 equal phases. The phase ϕ is defined by $\phi = t/T_0 - n$, where n is an integer such that $0 \leq \phi < 1$, where T_0 is the bar passing period for $F_{red} = 0.61$. The space-time diagrams of wall shear stress τ_w on the suction side are shown in figure 5. In figure 5 (a) and (b), the 'red' regions of high wall shear from leading edge to 0.6 are the response of the laminar boundary layers to the passage of the incoming wakes. The negative value marked in dashed lines indicate

the evolution of the separation bubbles. At $F_{red} = 0.31$ the separation region is larger than that of $F_{red} = 0.61$ case, corresponding to a larger wake loss generation discussed above.

4 Conclusions

Direct numerical simulations of the compressible flow pass through a low pressure turbine have been conducted to study the effect of incoming wakes generated by moving bars at different reduced frequencies as well as the combined effect with 4% inflow turbulence level. The results compare favorably with the reference data in terms of the pressure distributions and wake losses. It is evident that with the increment of reduced frequency, the wake loss is dramatically reduced and the influence of the inflow turbulence level is less significant in $F_{red} = 0.61$ case. The space-time diagrams of wall shear stress also show that the separation bubble can be suppressed effectively by the incoming wakes, especially at higher reduced frequency case.

References

1. Coull, J.D., Hodson, H.P.: Unsteady boundary-layer transition in low-pressure turbines. J. Fluid Mech. **681**, 370–410 (2011)
2. Engber, M., Fottner, L.: The effect of incoming wakes on boundary layer transition of a highly loaded turbine cascade. AGARD-CP-571 (1996)
3. Stieger, R.D., Hodson, H.P.: The Unsteady Development of a Turbulent Wake Through a Downstream Low-Pressure Turbine Blade Passage. J. Turbomach. **127**(2), 388–394 (2005)
4. Wu, X., Durbin, P.A.: Evidence of longitudinal vortices evolved from distorted wakes in a turbine passage. J. Fluid Mech. **446**, 199–228 (2001)
5. Michelassi, V., Wissink, J., Rodi, W.: Analysis of DNS and LES of flow in a low pressure turbine cascade with incoming wakes and comparison with experiments. Flow, Turb. & Comb. **69**, 295–330 (2002)
6. Sarkar, S.: Influence of wake structure on unsteady flow in a low pressure turbine blade passage. J. Turbomach. **131**(4), 041016 (2009)
7. Touber, E., Sandham, N.D.: Large-eddy simulation of low-frequency unsteadiness in a turbulent shock-induced separation bubble. Theor. & Comput. Fluid Dynamics **23**(2), 79–107 (2009)
8. Sandberg, R.D., Pichler, R., Chen, L.W.: Assessing the sensitivity of turbine cascade flow to inflow disturbances using direct numerical simulation. In: ISUAAAT 13, Tokyo, Japan, September 11-14 (2012)
9. Stadtmüller, P.: Investigation of wake induced transition on the LP turbine cascade T106A-EIZ. DFG-Verbundprojekt Fo, 136/11, Version 1.0, University of the Armed Forces Munich, Germany (2001)
10. Goldstein, D., Handler, R., Sirovich, L.: Modeling a no-slip flow boundary with an external force field. J. Comput. Phys. **105**, 354–366 (1993)